

# A geometrical investigation the effect of volumetric chip expansion factor in orthogonal turning processes

Zülküf DEMİR<sup>1</sup>

<sup>1</sup>Faculty of Engineering, Department of Mechanical Engineering, Batman University, Turkey

## Abstract:

Chip morphology is the remnant of the machining processes, providing to examine the quality of the machinability. The shape of the chip and its deformation rate identifying the severe of the processes outcomes, such as surface quality, tool life, required cutting forces and power. Especially, plastic deformation in the primary deformation zone makes the volume of the chip increase. The shear angle ( $\phi$ ), tool cutting edge approach angle ( $\gamma$ ), and chip thickness ( $t$ ) are the most influential parameters on the volumetric chip expansion factor ( $r_1$ ), in primary deformation zone. While tool cutting edge angle ( $\gamma$ ) has a correlate proportional effect, shear angle ( $\phi$ ) and chip thickness ( $t$ ), inversely proportional effect, on the volumetric chip expansion factor. According to getting the optimum volumetric chip expansion factor ( $r_1$ ), the lower tool cutting edge angles and feed rates, but higher shear angle must be selected. Rake angle ( $\alpha$ ) and cutting depth ( $a$ ) have not remarkable effect on the volumetric chip expansion factor ( $r_1$ ), but it only provides the sliding of the chip on the tool rake face.

**Keywords:** chip expansion factor, shear angle, approach angle, chip thickness, feed rate

## 1. Introduction

When you submit your paper print it in two-column format, including figures and tables. In addition, designate one author as the “corresponding author”. This is the author to whom proofs of the paper will be sent. Proofs are sent to the corresponding author only. The chip morphology is a vital indicator to demonstrate the quality of the machinability, according to the tool life, surface roughness, process temperature, required cutting forces and power criterion. Especially, chip morphology is depending on the contacting relationship between the cutting tool and workpiece. The removed chip gets its formation relative to this relationship, affected by the geometry of the tool, created by rake and clearance angles. Moreover, chip morphology affects the tool wear, caused by the flowing of the chip on the rake face (Ye et al., 2018; Atlati et al., 2011; Uzun et al., 2016; Bäker, 2003). While, the shape of the removed chip has an important marker to the cutting speed and feed rate, there is unimportant effect of the rake angle, in the primary shear zone. However, the rake angle provides shaping the chip segmentation in the secondary deformation zone,

where the cut chip flows (Arrazola et al., 2007). After the uncut chip is sustained to plastic deformation by the cutting edge of the tool, then it is removed from the workpiece. Moreover, the deformation makes the flow chip in serrated form, which is a challenging problem to solve in machining, in the primary zone. The serrated chip is created by the effect of inertia of thermal softening, strain hardening, elastic unloading, viscous and thermal diffusions, and power law between the serration frequency and Reynolds thermal number. Moreover, the serration frequency is a function of the cutting speed, namely increases in cutting speed causes to remove chips from the workpiece in serration form, also the serrated chip form is ascribed to the plastic shear instability in the primary shear zone, as well. Therefore, shear angle has vital influent on the plastic deformation, chip expansion factor or chip compression factor and removing the uncut chip from the workpiece in machining. Higher shear angles provide lower chip expansion factor. With increasing rake angle shear angle increases linearly in primary deformation zone (Ye et al., 2014; Weber et al., 2007; Kishawy et al., 2002; Ijaz et al., 2017; Lampart, 2009). The most influential

parameters on the plastic deformation of the uncut chip are shear angle, tool approach angle, rake angle, depth of cut, and feed rate, namely chip thickness. Furthermore, these parameters affect the chip expansion, therefore, the chip expansion factor is an important identifier for the machinability. There is an inversely proportional relationship between the shear angle and chip expansion factor. At higher chip expansion factors and shear angles, the effect of rake angle decreases or disappears totally on the chip formation in machining processes (Kronenberg, 1996).

The contact length, the sticking, and sliding region in the chip-tool interface depend on parameters such as tool geometry and edge preparation. High stress is appeared in the primary deformation zone, while the equivalent stress in the cutting tool is identified by the rake angle and the cutting edge preparation (Ashwin et al., 2017). The stress decreases with increasing feed rate, but the tool stress is dissipated in a larger area in tool-chip interface. However, at lower feed rates the stress is influential in a smaller area due to the contact length of the tool and chip (Ijaz et al., 2017). Furthermore, with increasing feed rate the frequency of the chip segmentation decreases, ending up with serrated chip, but negative rake angles causes larger plastic strain (Arrazola et al., 2007). However, increases in the cutting speed there is an inclination to support provisional chip shaping (Ye et al., 2014). The magnitude of the stress in machining processes is depending on elastic and shear modulus in different directions (Arif, 2017). Furthermore, the stresses in machining operations are caused by the temperature, taking place, during the metal cutting. This temperature affects the layer near the machined surface and causes the chip expansion and plastic flow (Migueluez et al., 2009; Liu et al., 2017). Orthogonal cutting, in which selected feed rates too smaller than the depth of the cut, prevents the severe deformation in the perpendicular direction, with the help of the pressure between the cutting edge and the workpiece (Buchkremer and Schoop, 2016).

The tool cutting edge geometry and inclination angles, especially rake angle has a vital effect on shaping of the removed chip on the tool rake face, in the secondary deformation zone (Izaj et al., 2017). While the negative rake angles provide chips removed in the short form, the positives in the continuous (Weber et al., 2007). Moreover, the undeformed chip thickness has an influence on the

removed chip, shaping in continuous, brittle, and serrated forms. However, the effect of the cutting speed and feed rate is more severe than undeformed chip thickness on the shaping of the removed chips (Lampart, 2009).

Mechanical and thermal conditions are the actual boundary machining conditions. Cutting direction demonstrable orthogonal or oblique, and feed rate create the mechanical conditions, but the chip segment length is independent on the cutting speed and tool geometry (Bäker, 2003). The repeated shear band in primary zone provides changing the flowing chip shape from serrated to continuous. However, the serrating chip formation depends on the mechanical properties of the workpiece, as well (Weber et al., 2007). Serrated chips are removed from the machined sample in saw-tooth form. The pitch of the teeth demonstrates the severe of the fluctuation in cutting forces. At large feed rates, while the dimension of saw-teeth decreases, the number of them increases. The most influential parameter on the serrated, saw-tooth chip morphology is the initial chip thickness. Increases in cutting speed results in changing chip formation from continuous to serrated, hence the cutting speed is an important marker for the serrating chip morphology and strain rate, making the material brittle (Kronenberg, 1996).

Because of its economic and technical significance, the chip formation has been commonly analyzed. The quality of the machining process can be identified relative to the chip plastic deformation, commonly affected by the shear angle, cutting edge approach angle, feed rate, namely chip thickness, depth of cutting, and rake angle. Chip expansion factor displays the rate of the deformation of the uncut chip during the machining process. Therefore, this factor identifies the quality of the machinability, according to the process results such as surface quality and tool life. For this purpose, in this theoretical study, chip expansion factor was analyzed geometrically depending on shear, rake, deformation, cutting edge approach angles, feed rate, and depth of cutting, for turning operations.

## **2. Analyzing the chip expansion factor geometrically**

Chip morphology is a vital phenomenon in machining operation, demonstrating the quality of the process. Uncut chip sustains to plastic deformation then it is removed from the workpiece.

The level of the plastic deformation identifies the results of the process, such as surface roughness, tool life, required cutting forces and power, etc. Therefore the chip expansion factor has an important effect on the machining operations. Any point on the cutting edge of the tool travels on the workpiece, as feed rate ( $f$  (mm/rev)), while the

cylindrical workpiece revolves a cycle, in turning operations, as shown in Figure 1 a. In the circumstances the chip removed from the workpiece has three dimension as feed rate ( $f$  (mm/rev)) or chip thickness ( $t$  (mm)), cutting depth ( $a$  (mm)) or chip wide ( $b$  (mm)), and chip length ( $l$  (mm)) in a cycle of the workpiece as seen in Figure 1 b.

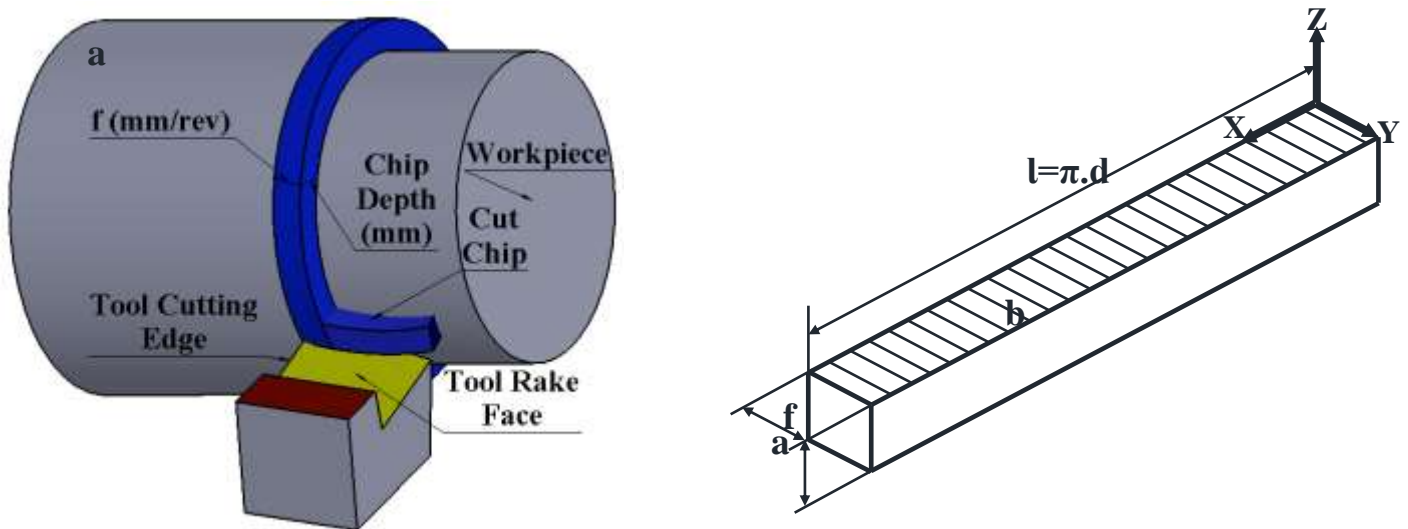


**Figure 1:** The removed chip geometrical dimensions and volume in a cycle of the workpiece, a) machining mechanism in turning, b) the removed chip dimensions in a cycle of the sample.

If it is accepted the shear angle were equal to zero, while the chip was removed from the workpiece by the cutting tool, the removed chip dimensions: chip thickness or feed rate, depth of cut or chip wide, and chip length were equal to  $f$  (mm/rev) or  $t$  (mm),  $a$  (mm) or  $b$  (mm),  $l$  (mm), respectively. In the present case, The volume of the chip, removing from the

workpiece in a cycle as seen in Figure 1, calculable as seen in Equation 1.

$$V_1 = a \cdot f \cdot l \quad (1)$$

Additionally, this volume ( $V_1$ ) is equal to the volume of the uncut chip, limiting among (ABCDEFGH), as shown in Figure 2.

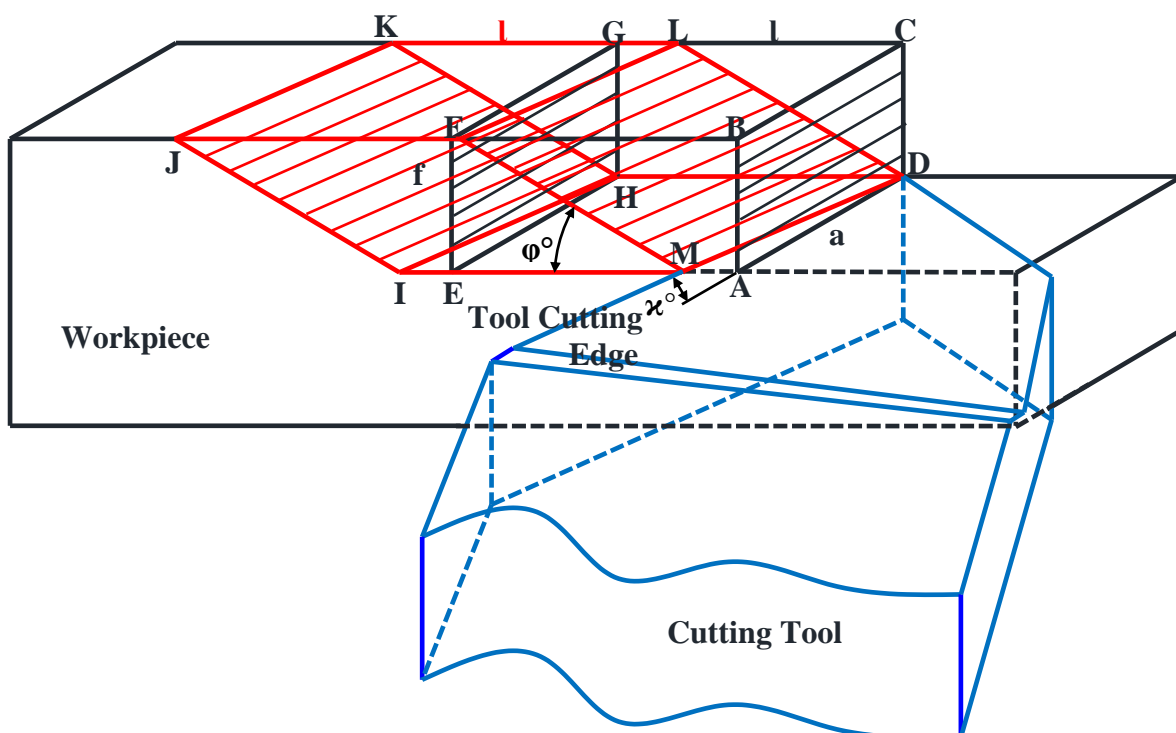


**Figure 2:** The chip removing mechanism in turning operations in primary deformation zone.

The volume of the removed chip calculable with using  $|DM|$ ,  $|FM|$ , and  $|JF|$  edges dimensions as shown in Equation 2. It is accepted that during the cutting process, there is not any deformation effect on the edges of the removed chip, at boarding among (FGDMIJKH). The volume of the removed chip ( $V_2$ ), limiting among (FGDMIJKH), computable as seen in Equation 3. The removed chip, demonstrating in Figure 2 with limiting (FGDMIJKH), only the effect of shearing ( $\phi$ ) and tool cutting edge approaching (side cutting edge)

angles was taken into account.

$$|DM| = \frac{a}{\cos\chi}, |FM| = \frac{f}{\sin\phi}, |JF| = |KG| = 1, \quad (2)$$

$$V_2 = \int_0^1 \int_0^\phi \int_0^\chi J_v \, d\chi \, d\phi \, dl \quad (3)$$

The Jacobian of conversion factor ( $J_v$ ) of the volume equation can be identified as in Equation 4.

$$J_v = \begin{bmatrix} \frac{\partial |DM|}{\partial \chi} & \frac{\partial |DM|}{\partial a} \\ \frac{\partial |FM|}{\partial \phi} & \frac{\partial |FM|}{\partial f} \end{bmatrix} = \begin{bmatrix} \frac{a \cdot \sin\chi}{\cos^2\chi} & \frac{1}{\cos\chi} \\ \frac{f \cdot \cos\phi}{\sin^2\phi} & \frac{1}{\sin\phi} \end{bmatrix} \Rightarrow J_v = \frac{a \cdot \sin\chi}{\sin\phi \cdot \cos^2\chi} - \frac{f \cdot \cos\phi}{\cos\chi \cdot \sin^2\phi}$$

(4)

In the circumstances,  $V_2$  chip volume computable as Equation 5.

$$V_2 = \int_0^1 \int_0^\phi \int_0^\chi \frac{a \cdot \sin\chi}{\sin\phi \cdot \cos^2\chi} - \frac{f \cdot \cos\phi}{\cos\chi \cdot \sin^2\phi} \, d\chi \, d\phi \, dl \Rightarrow$$

$$V_2 = l \cdot \left[ -\frac{a}{\cos\chi} \cdot \ln\left(\frac{1}{\cos\phi} - \cot\phi\right) - \frac{f}{\cos\phi} \cdot \ln\left(\frac{1}{\cos\chi} + \tan\chi\right) \right]$$

(5)

Actually, when the chip removed from the machining workpiece by using a turning machine, the chip edges, near to the cutting edge of the tool, as seen in Figure 3, as  $|FB|$  and  $|BC|$  are deformed by the effect of the cutting edge compression. Because when the uncut chip is subjected to the compression effect, the counter reaction forces ( $F_t$ ) resulted in as shown in Figure 3. On  $\eta$  and  $\pi$  planes. Therefore, two edges of the chip  $|FAI|$  and  $|AIC|$  change as  $|FB|$  and  $|BC|$  edges, by the effect of the compression strength, shear ( $\phi$ ), and cutting edge approach ( $\chi$ )

angles. However, the chip thickness, shaping by the effect of the feed rate motion, change from  $|BH|$  to  $|BHI|$  by the effect of tensile strength. Furthermore, these edges of the chip deform under the compression strength and the one tensile strength.

If it is accepted  $\beta_0$ ,  $\rho_0$ , and  $\delta_0$  angles, in Figure 3, are equal to zero (0). In other words, the effect of these angles are neglected, the volume of the removed chip can be calculated as shown in Equations from 6 to 10.

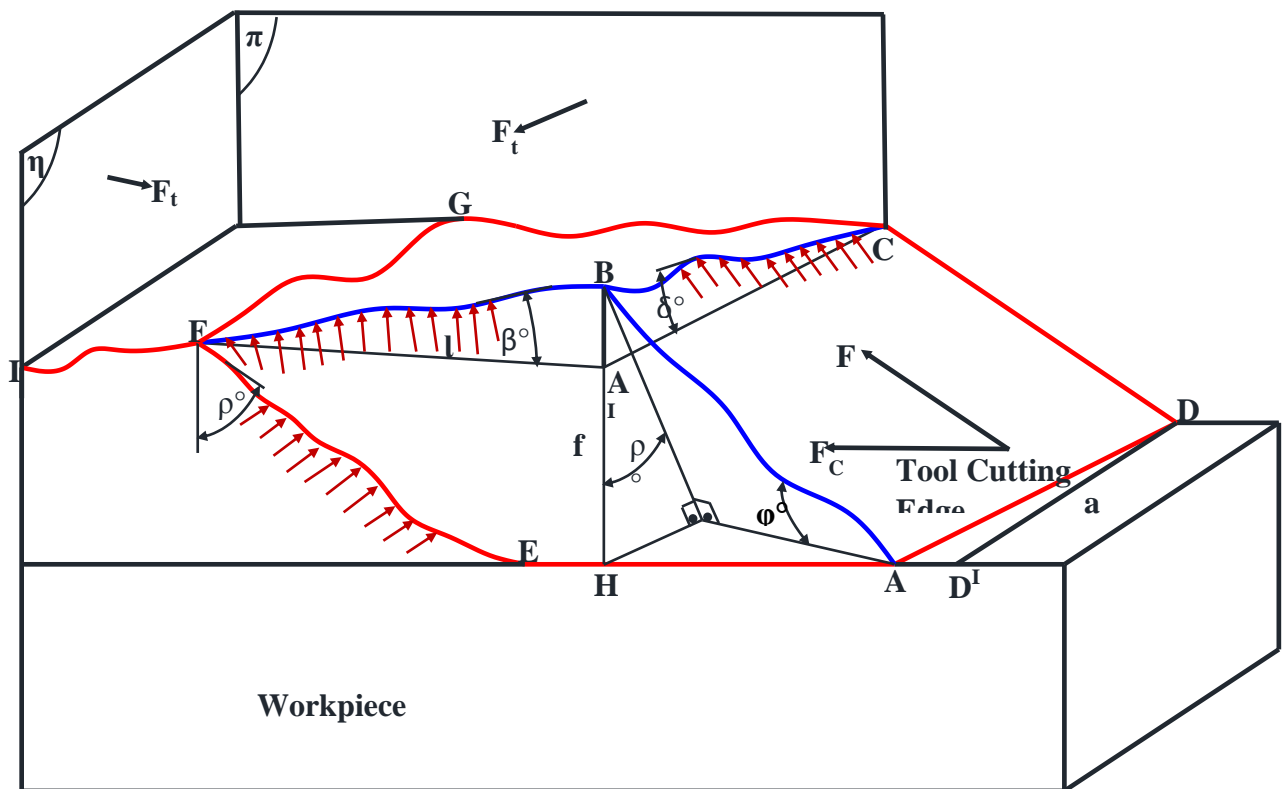


**Figure 3:** The mechanism of the deformation of the edges of the removed chip.

In Figure 4, the length of the  $|FB|$  or  $|EA|$  is equal to the uncut chip length, in one cycle of the workpiece, during turning processes. After the chip was cut from the workpiece by the cutting edge, in the primary deformation zone, then it was moved on the rake face of the tool in the secondary deformation zone. The uncut chip length  $|FB|$  or  $|EA|$  is transited from primary to secondary deformation zones. When the tool rake angle ( $\alpha$ ) equals to zero, the uncut chip length is located on  $\varepsilon$  plane in secondary deformation zone.

$$V_3 = \int_0^{\alpha} \int_0^{\phi} \int_0^{\chi} J_v \, d\chi \, d\phi \, d\alpha \quad (6)$$

At the beginning of the machining process, the chip, cuts by the cutting edge of the tool, removes from the workpiece, in the primary deformation zone,

$$|BC| = \frac{a}{\cos\chi}, \quad |B^1A^1| = \frac{f \cdot \cos(\phi - \alpha)}{\sin\phi}, \quad |AA^1| = \frac{l}{\cos\alpha}, \quad (7)$$

In Figure 4,  $\varepsilon$  is the vertical plane in the directions of Z and Y. Moreover,  $\theta$  is the plane of the rake face of the cutting tool. The conversion factor (JV) of the

then it moves on the rake face of the tool in the inclination of rake angle ( $\alpha$ ), as seen in Figure 4, limiting among ABCDAIBICIDI. In the circumstances, the volume of the chip, moving on the rake face of the tool, can be calculated by using Equation 9.

According to the Figure 4  $|BC|$ ,  $|BIAI|$ , and  $|AAI|$  lengths calculable depending on cutting depth ( $a$ ), chip thickness ( $f$ ), chip length ( $l$ ), cutting edge approach angle ( $\chi$ ), shear angle ( $\phi$ ), and rake angle ( $\alpha$ ) as seen in Equation 7.

chip volume can be calculated, as in Equation 8, by using Jacobian method.

$$J_v = \begin{bmatrix} \frac{\partial |BC|}{\partial \chi} & \frac{\partial |BC|}{\partial a} & 0 \\ \frac{\partial |B'A'|}{\partial \phi} & \frac{\partial |B'A'|}{\partial \alpha} & \frac{\partial |B'A'|}{\partial f} \\ \frac{\partial |DM|}{\partial \alpha} & \frac{\partial |DM|}{\partial l} & 0 \end{bmatrix} \Rightarrow$$

$$J_v = \begin{bmatrix} \frac{a \cdot \sin \chi}{\cos^2 \chi} & \frac{1}{\cos \chi} & 0 \\ -f \cdot \cos \alpha & f \cdot (\cos \alpha - \cot \phi \cdot \sin \alpha) & \frac{\cos(\phi - \alpha)}{\sin \phi} \\ l \cdot \frac{\sin \alpha}{\cos^2 \alpha} & \frac{1}{\cos \alpha} & 0 \end{bmatrix}$$

(8)

$$V_3 = \int_0^\alpha \int_0^\phi \int_0^\chi \left( l \cdot \frac{\sin \alpha}{\cos^2 \alpha \cdot \cos \chi} \cdot \frac{\cos(\phi - \alpha)}{\sin \phi} \right) - \left( \frac{a \cdot \sin \chi}{\cos^2 \chi \cdot \cos \alpha} \cdot \frac{\cos(\phi - \alpha)}{\sin \phi} \right) d\chi d\phi da$$

$$\Rightarrow$$

$$V_3 = l \cdot \left( \ln\left(\frac{1}{\cos \chi} + \tan \chi\right) \cdot \ln(\sin \phi) \cdot \ln\left(\frac{1}{\cos \chi}\right) + \tan \alpha - 1 \right) - \left( \frac{a}{\cos \chi} \cdot \ln(\sin \phi) + \ln\left(\frac{1}{\cos \alpha}\right) \right)$$

(9)

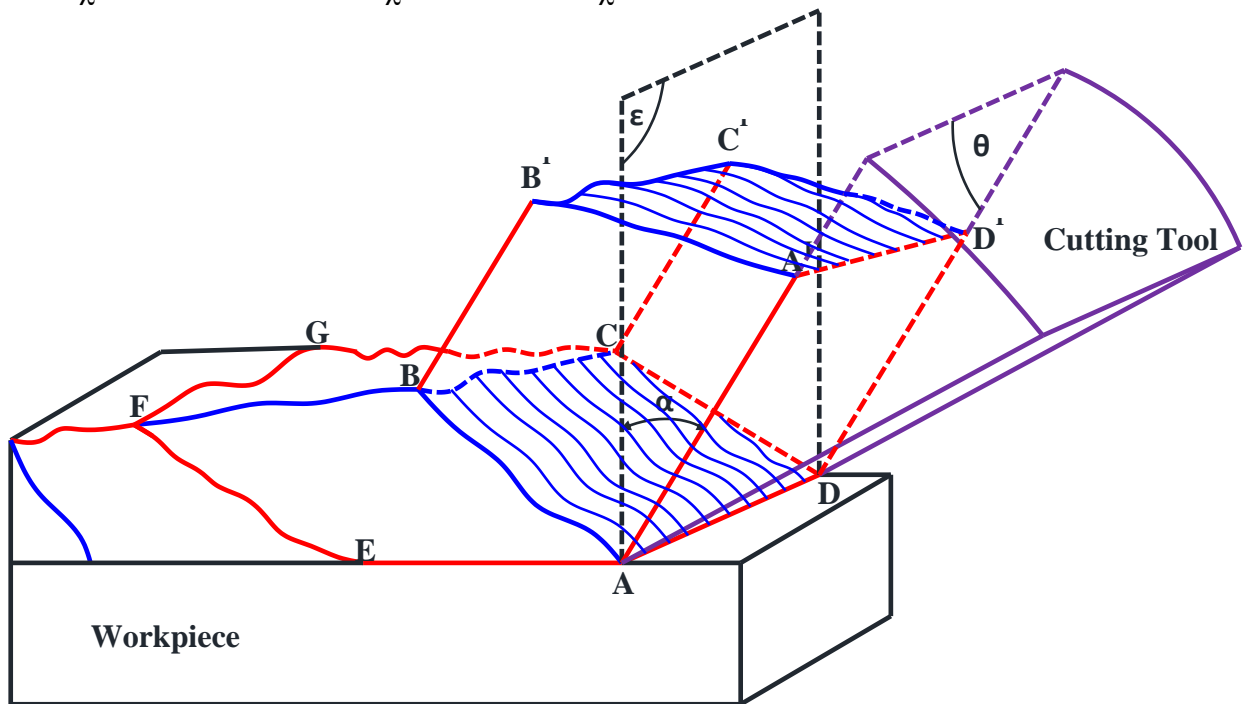


**Figure 4:** The chip, removed from the workpiece, then moves on the rake face in the secondary zone.

As seen in Fig. 8, the part of the chip, limiting among (ABCD A I I B I I C I I D I I), has an inclination angle ( $\gamma$ ) with ( $\psi$ ) plane, on the rake face of the tool. In the circumstances, the effect of deformation angle ( $\gamma$ ) on the volume of the chip can be calculated as in Equations from 10 to 14.

$$V_4 = \int_0^\gamma \int_0^\phi \int_0^\chi J_v d\chi d\phi d\gamma$$

(10)

$$|BC| = |B''C''| = \frac{a}{\cos \chi}, |B''A''| = \frac{f \cdot \cos(\phi - \alpha)}{\sin \phi}, |AA''| = \frac{l}{\cos \alpha \cdot \cos \gamma},$$

(11)

$$J_v = \begin{bmatrix} \frac{\partial |B''C''|}{\partial \chi} & \frac{\partial |B''C''|}{\partial a} & 0 \\ \frac{\partial |B''A''|}{\partial \varphi} & \frac{\partial |B''A''|}{\partial \alpha} & \frac{\partial |B''A''|}{\partial f} \\ \frac{\partial |AA''|}{\partial \alpha} & \frac{\partial |AA''|}{\partial \gamma} & \frac{\partial |AA''|}{\partial l} \end{bmatrix} \Rightarrow$$

$$J_v = \begin{bmatrix} \frac{a \cdot \sin \chi}{\cos^2 \chi} & \frac{1}{\cos \chi} & 0 \\ f \cdot \frac{\cos(2\varphi - \alpha)}{\sin^2 \varphi} & f \cdot \frac{\sin(\varphi - \alpha)}{\sin \varphi} & \frac{\cos(\varphi - \alpha)}{\sin \varphi} \\ l \cdot \frac{\sin \alpha}{\cos^2 \alpha \cdot \cos \gamma} & \frac{l \cdot \sin \gamma}{\cos \alpha \cdot \cos^2 \gamma} & \frac{1}{\cos \alpha \cdot \cos \gamma} \end{bmatrix}$$

(12)

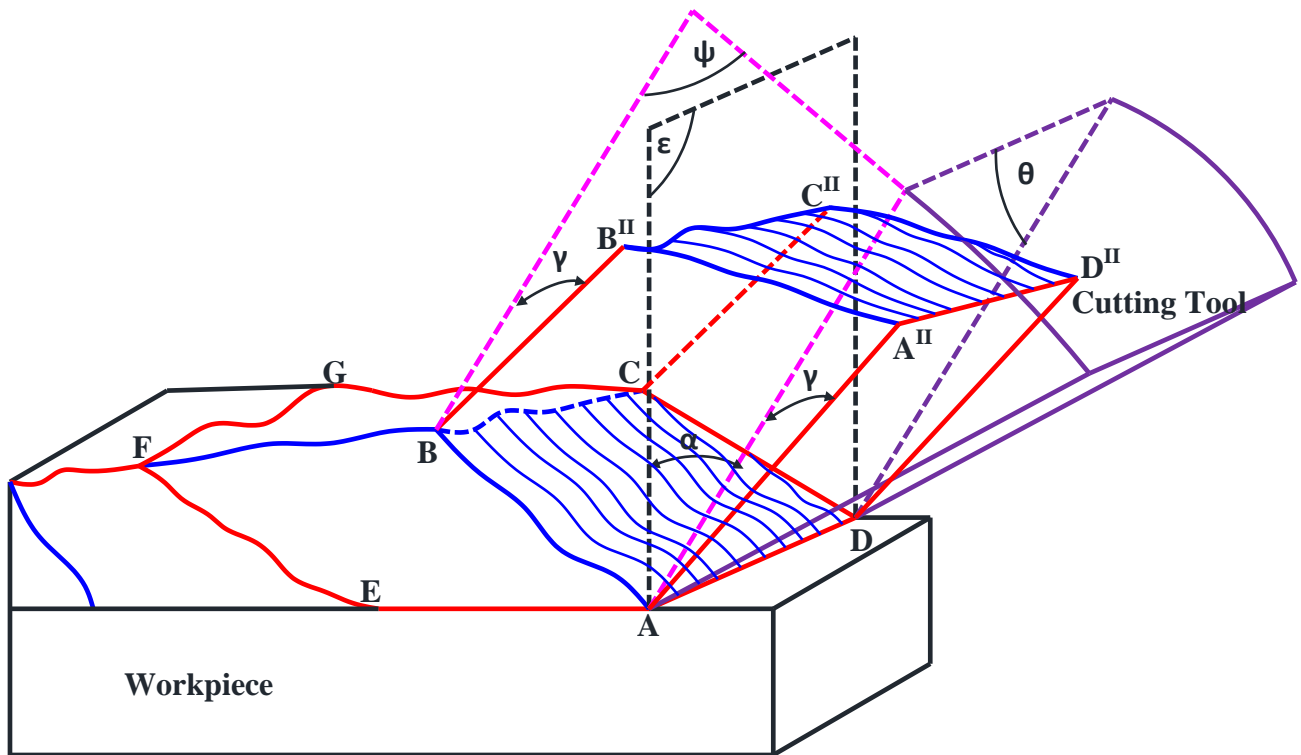


**Figure 5:** The chip deformation angle on the rake face of the tool, in the secondary deformation zone.

$$V_4 = \int_0^{\gamma} \int_0^{\varphi} \int_0^{\chi} (w-y) d\chi d\varphi d\gamma$$

(13) The values of  $w$  and  $y$  are written depending on selected parameters as at below. With solving the Equation 13 by taken the integral, Equation 14 derivable.

$$w = \left[ a \cdot f \cdot \frac{\sin \chi}{\cos^2 \chi} \cdot \frac{(1 - \cot \varphi \cdot \tan \alpha)}{\cos \gamma} \right] + \left[ l \cdot \frac{\sin \alpha}{\cos^2 \alpha \cdot \cos \chi \cdot \cos \gamma} \cdot (\cot \varphi \cdot \cos \alpha + \sin \alpha) \right]$$

$$y = \left[ a \cdot l \cdot \frac{\sin \chi}{\cos^2 \chi} \cdot \frac{\sin \gamma}{\cos^2 \gamma} \cdot (\cot \varphi + \tan \alpha) \right] + \left[ \frac{(\cot^2 \varphi - 1) + \sin 2\varphi \cdot \tan \alpha}{\cos \chi \cdot \cos \gamma} \right]$$

$$V_4 = z + p + s$$

(14)

The values of z, p, and s are written depending on selected parameters as at below.

$$z = \left[ \frac{a \cdot f}{\cos \chi} \cdot \ln \left( \frac{1}{\cos \gamma} + \tan \gamma \right) \cdot (\varphi - \tan \alpha \cdot \ln(\sin(\varphi))) \right]$$

$$p = \left[ \frac{l \cdot \sin \alpha}{\cos \gamma} \cdot \ln \left( \frac{1}{\cos \gamma} + \tan \gamma \right) \cdot \ln \left( \frac{1}{\cos \chi} + \tan \chi \right) \cdot (\ln(\sin(\varphi)) \cdot \cos \alpha + \varphi \cdot \sin \alpha) \right]$$

$$s = \left[ \left( \cot \varphi + \frac{\cos 2\varphi}{2} \cdot \tan \alpha + 2 \right) \cdot \ln \left( \frac{1}{\cos \chi} + \tan \chi \right) \cdot \ln \left( \frac{1}{\cos \gamma} + \tan \gamma \right) \right] - \left[ \frac{a \cdot l}{\cos \chi \cdot \cos \gamma} \cdot (\ln(\sin(\varphi)) + \varphi \cdot \tan \alpha) \right]$$

Furthermore, instead of deformation angle ( $\gamma$ ) its value can be written, depending on shear and rake angles, as seen in Equation 15 (Michael, 1996).

$$\gamma = \cot \varphi + \tan(\varphi - \alpha)$$

(15)

The volumetric chip expansion factor in primary deformation zone ( $r_1$ ) acquirable by dividing the chip volume ( $V_2$ ) (Equation 5) to ( $V_1$ ) (Equation 1), as shown in Equation 16.

$$r_1 = \frac{V_2}{V_1}$$

(16)

The volumetric chip expansion factor ( $r_1$ ) in secondary deformation zone on the tool rake face ( $r_2$ ) acquirable by dividing the chip volume ( $V_3$ ) (Equation 9) to ( $V_1$ ) (Equation 1), as shown in Equation 17.

$$r_2 = \frac{V_3}{V_1}$$

(17)

The volumetric chip expansion factor ( $r_1$ ) in secondary deformation zone on the tool rake face, taken place by the effect of deformation angle ( $R$ ) acquirable by dividing the chip volume ( $V_4$ ) (Equation 14) to ( $V_1$ ) (Equation 1), as shown in Equation 18.

$$R = \frac{V_4}{V_1}$$

(18)

### 3. Results and discussion

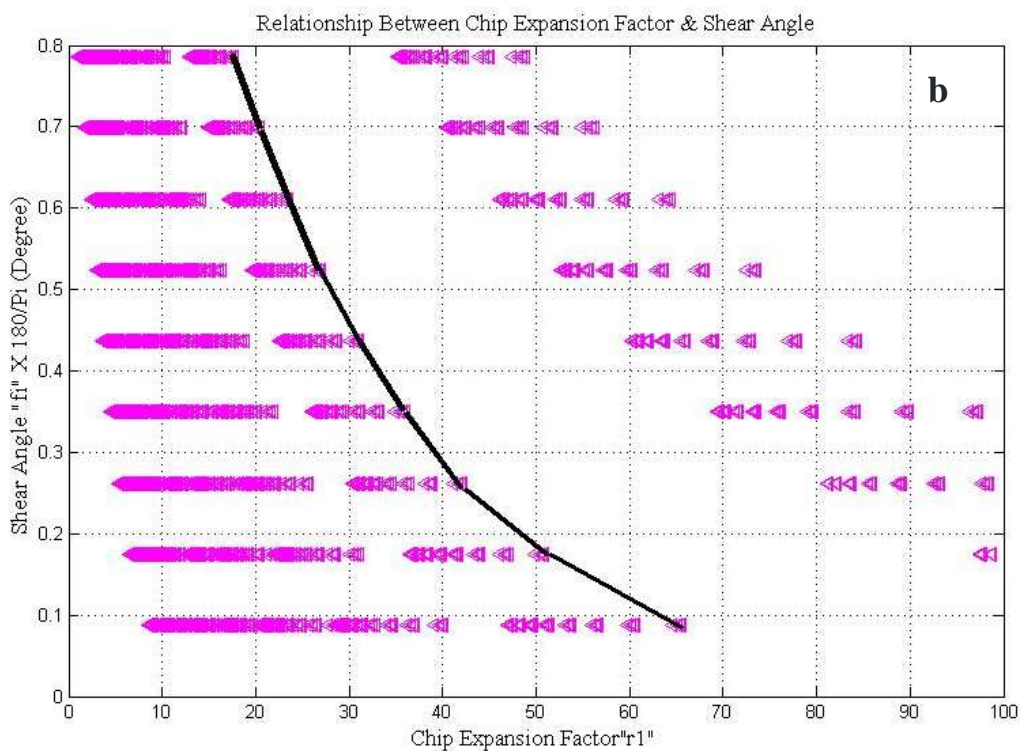
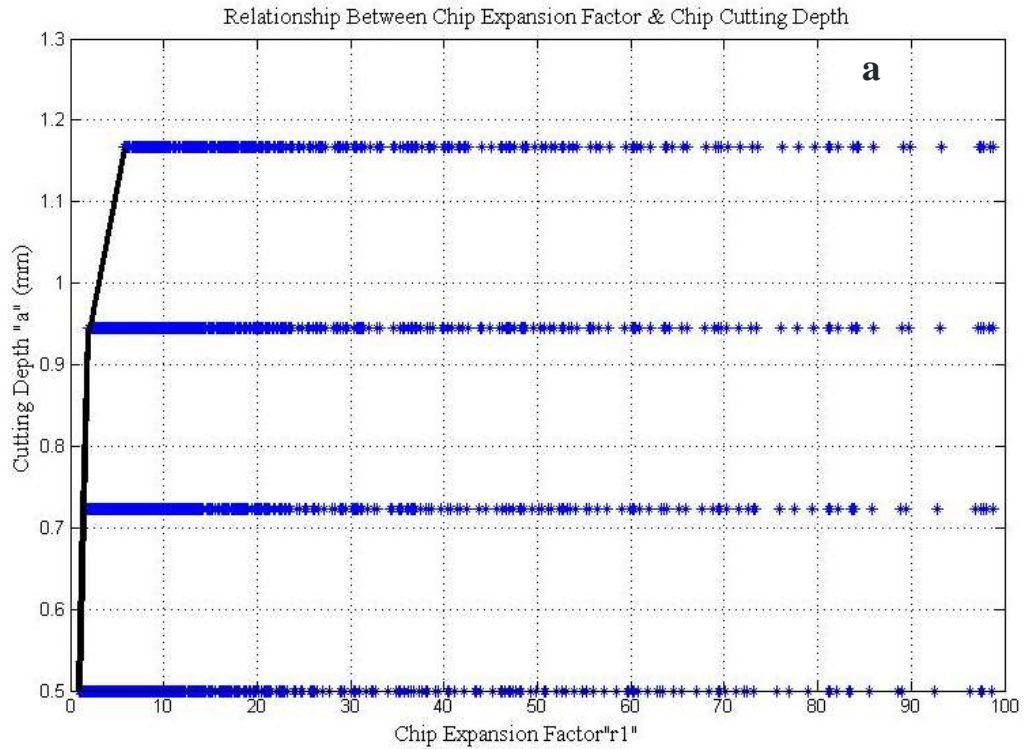
#### 3.1 Volumetric chip expansion factor ( $r_1$ ) in primary deformation zone

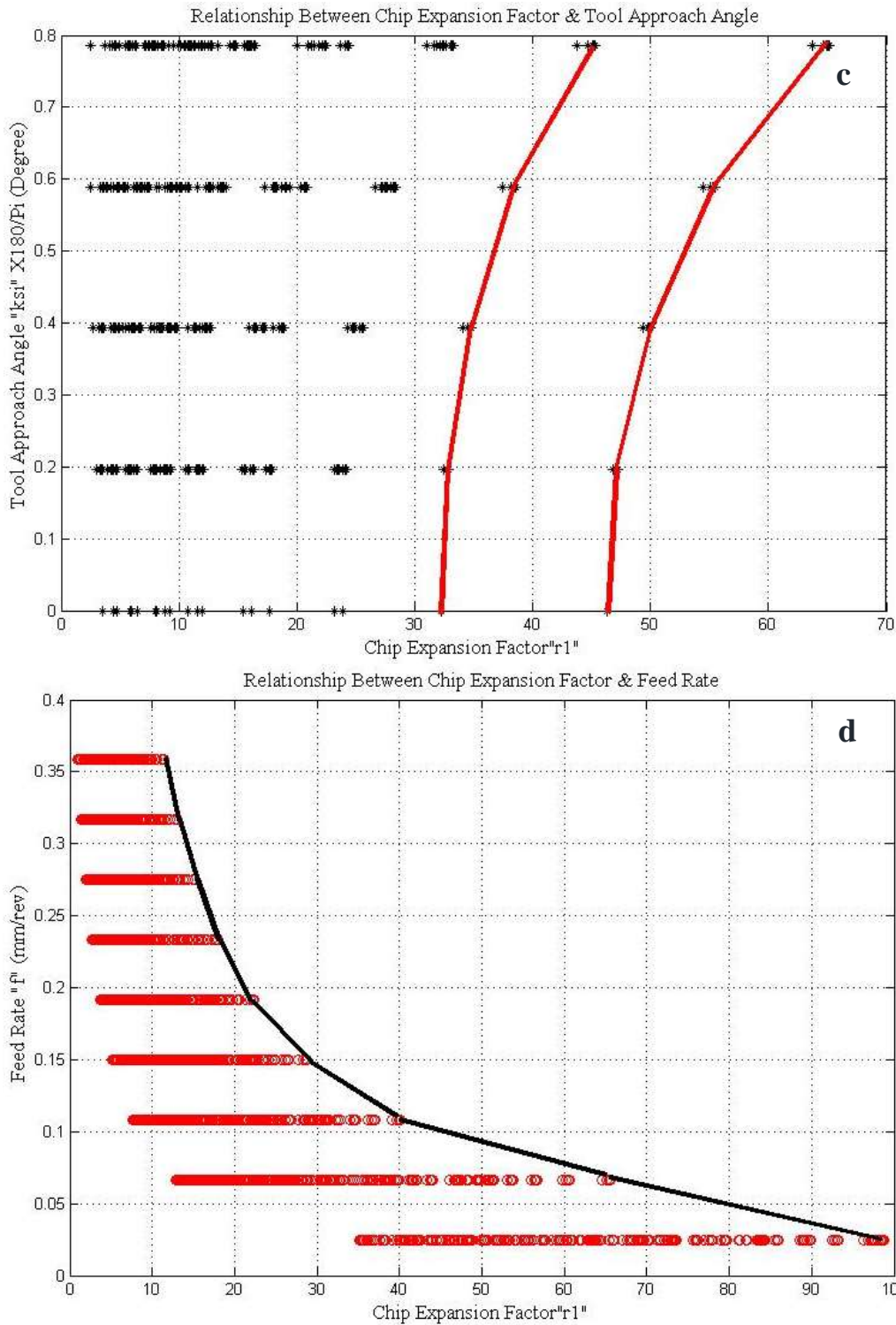
In the primary deformation zone, when the edge of the cutting tool contact to the workpiece, the uncut chip starts sustaining to plastic deformation, by the effect of shearing and other selected parameters, such as feed rate, depth of cut, tool approach angle, and rake angle. As seen in Figure 1 a, in one cycle of the workpiece the removed chip dimensions are chip thickness ( $t$ ) or feed rate ( $f$ ), depth of cutting ( $a$ ) or chip wide ( $b$ ), and chip length ( $l$ ) shown as in Figure 1 b.

The effect of shear angle, feed rate, cutting tool edge angle, and depth of cutting on the volumetric chip expansion factor ( $r_1$ ) were investigated geometrically, in primary deformation zone. For this purpose, shear angle ( $\varphi$ ) and cutting tool edge approach angle ( $\chi$ ) were selected between  $0^\circ - 45^\circ$ , feed rate ( $f$ )  $0.05 - 0.25$  (mm/rev), and depth of cutting  $0.5 - 2$  (mm). The effect of these parameters on the volumetric chip expansion factor ( $r_1$ ) was

investigated theoretically, by using by using Matlab software as seen in Figure 6.

The effect of cutting depth ( $a$ ), shear angle ( $\varphi$ ), cutting tool edge approach angle ( $\chi$ ), and feed rate ( $f$ ) on the volumetric chip expansion factor ( $r_1$ ) are seen as in Figure 6 a, b, c, and d, respectively. According to these graphs, in Figure 6, while the effect of shear angle and feed rate on the volumetric chip expansion factor ( $r_1$ ) is much bigger than the effect of cutting depth and cutting tool edge approach angle. As seen in Figure 6 a, the cutting depth has insignificant effect on the volumetric chip expansion factor ( $r_1$ ). However, the effect of both shear angle and feed rate have a vital inversely effect on the volumetric chip expansion factor ( $r_1$ ), namely with increasing shear angle and feed rate the volumetric chip expansion factor ( $r_1$ ) decreases. Moreover, increases in tool cutting edge approach angle causes the volumetric chip expansion factor ( $r_1$ ) to increase, as seen in Figure 6 c. In primary deformation zone, the most influential parameter is shear angle, following with feed rate, tool cutting edge approach angle, and depth of cutting, respectively.

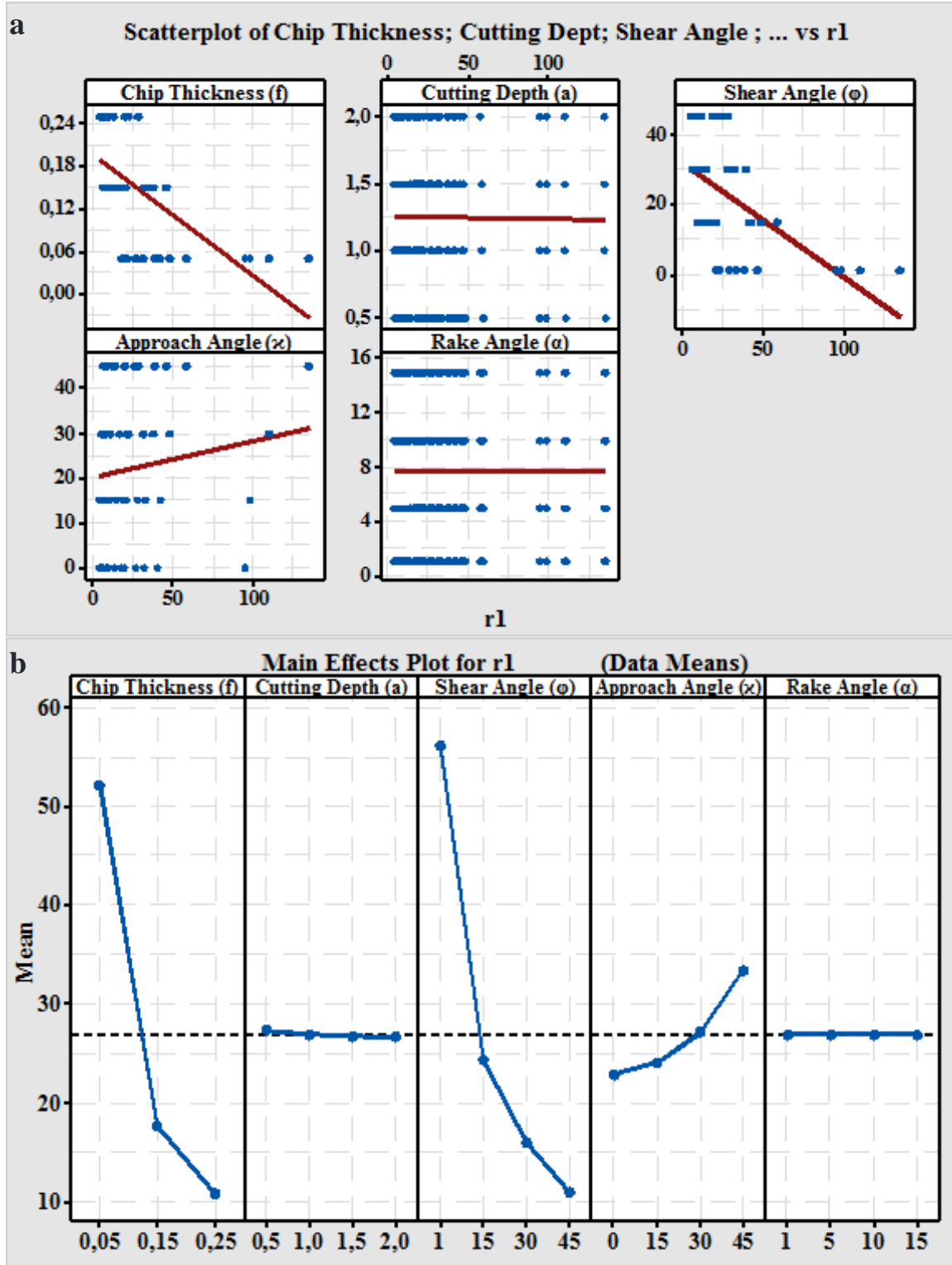


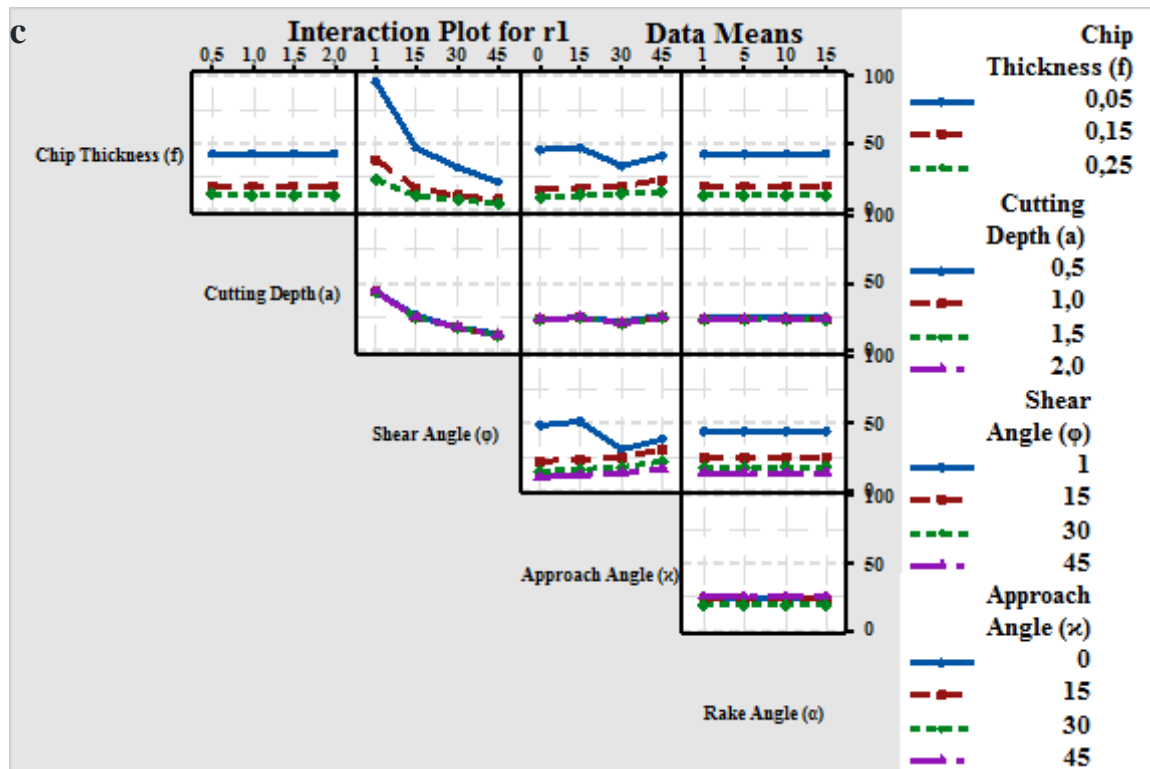


**Figure 6:** Matlab graphs of the effect of a) cutting depth, b) shear angle, c) approach angle, d) feed rate (chip thickness) on the chip expansion factor.

In Figure 7 a, b, and c, the scatter, main effect, and interaction plots of chip thickness (f), cutting depth (a), shear angle ( $\phi$ ), approach angle ( $\chi$ ), and rake angle ( $\alpha$ ), respectively. According to the scatter plot, while, rake angle has not any effect on the volumetric chip expansion factor (r1), the effect of cutting depth is too small to negligible. However, the approach angle has directly proportional, shear angle and feed rate inversely proportional effects on

the volumetric chip expansion factor (r1). In other words, with increasing tool cutting edge approach angle the volumetric chip factor (r1) increases linearly, but with increasing both shear angle and feed rate decreases inversely correlated. The main effect plot of the selected parameters, as seen in Figure 7 b, show the same changes correlated to the volumetric chip expansion factor (r1).

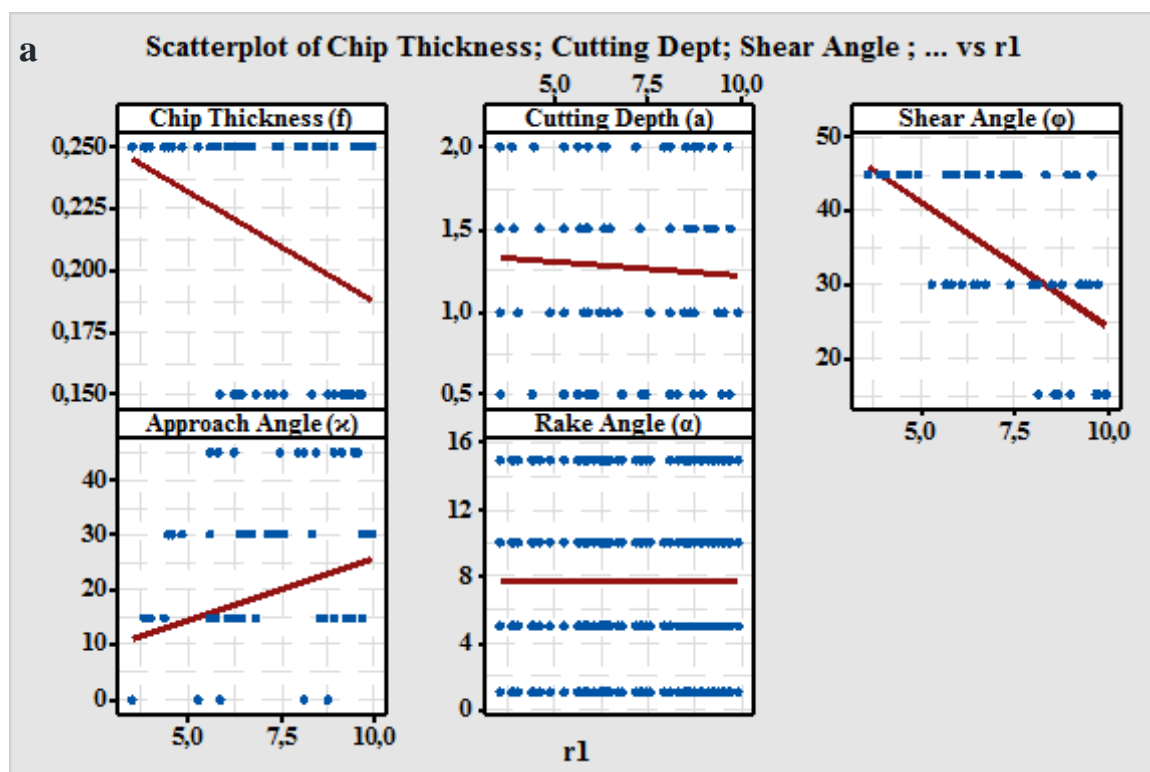




**Figure 7:** a) Scatterplot graphs, b) main effect plot, c) interaction plot of chip thickness, cutting depth, shear angle, approach angle, rake angle and chip expansion factor in the first deformation zone.

The interaction effect of parameters on the volumetric chip expansion factor is shown in Figure 7 c. Depending of the graphs, while chip thickness or feed rate, shear angle, and cutting edge approach

angle have important effect on the volumetric chip expansion factor, separately, but with interaction of cutting depth and feed rate their effect decreases too small to negligible.



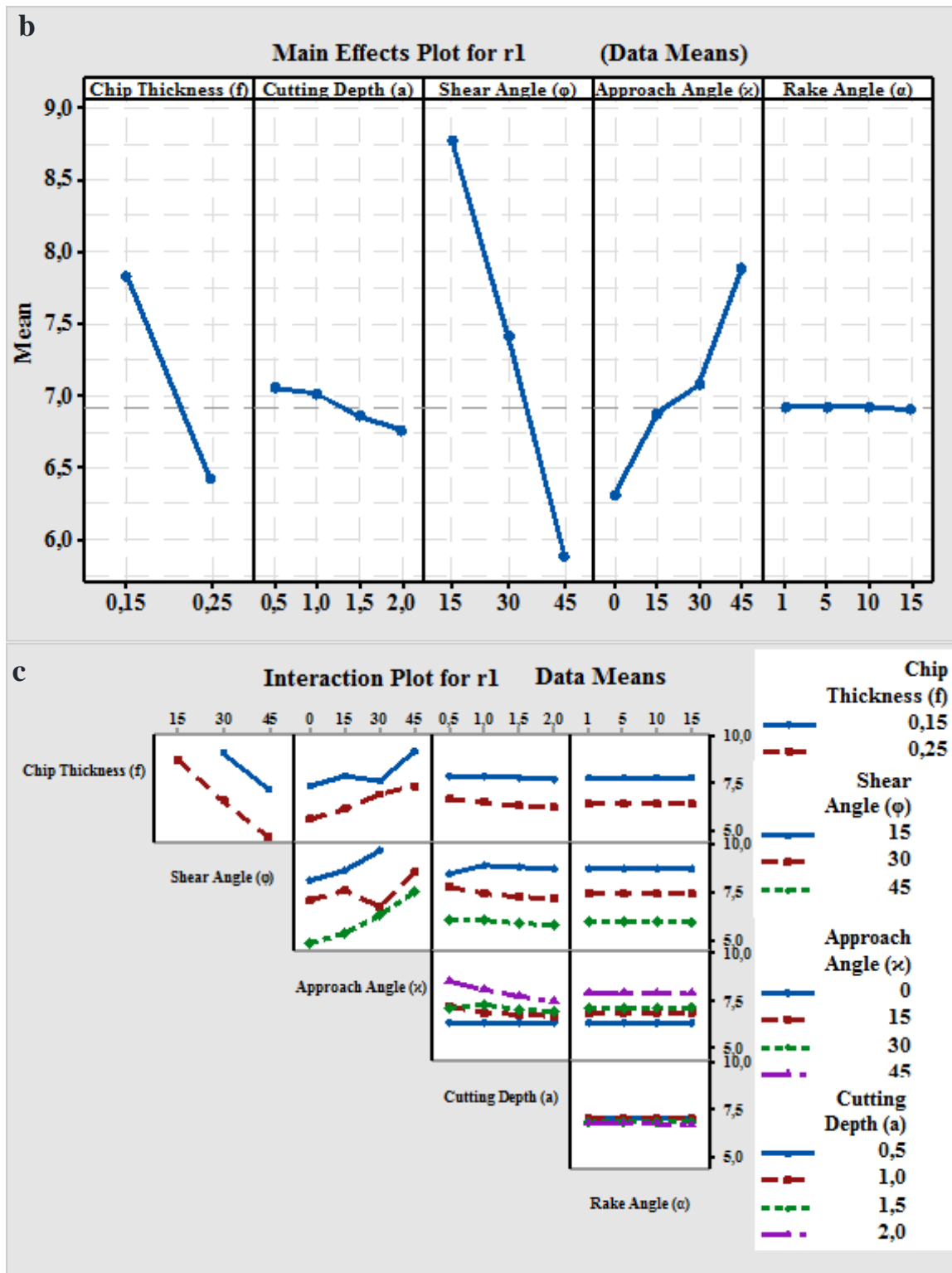


**Figure 8:** a) Scatterplot graphs, b) main effect plot, c) interaction plot of chip thickness, cutting depth, shear angle, approach angle, rake angle and chip expansion factor ( $r_1$ ) in the first deformation zone, for  $4 \leq r_1 \leq 10$  condition.

According to (Mustafa, 1996), volumetric chip expansion factor ( $r_1$ ) is an important outcome in machining operations, demonstrating the cutting conditions, surface quality, and chip morphology. Therefore, depending on these criterion, when ( $r_1$ ) is bigger than  $r_1 > 100$  is undesirable,  $31 \leq r_1 \leq 60$  limited appropriate,  $11 \leq r_1 \leq 30$  appropriate,  $4 \leq r_1 \leq 10$  excellent, and  $r_1 \leq 3$  well (Mustafa, 1996). Depending

on these criterion, the effect of parameters on the volumetric chip expansion factor ( $r_1$ ), in primary deformation zone, is as shown in Figure 8 a, b, and c. The most influential parameter are shear angle, cutting edge approach angle, and chip thickness, while there is too small to negligible effect of the cutting depth, but there is any effect of rake angle, according to scatter, main effect and interaction

plots, as seen in Figure 8 a, b, and c, respectively. As seen in Figure 8 c, for resulting in the optimum volumetric chip expansion factor ( $r_1$ ) values, the selected parameters provide the shear angle adjusted

to be between  $15^\circ - 45^\circ$ , higher feed rates between  $0.15 - 0.25$  (mm/rev), and cutting tool approach angle between  $0^\circ - 45^\circ$  can be selected, according to the interaction plot of parameters.

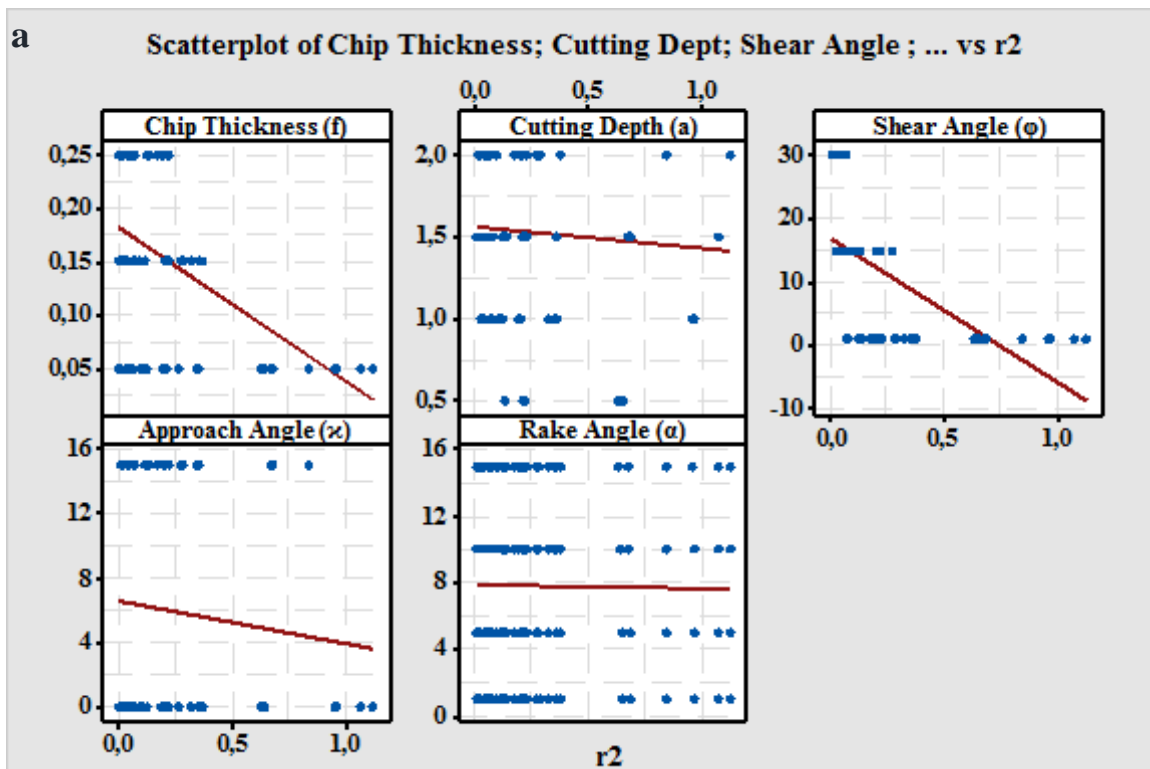
### 3.2 Volumetric chip expansion factor ( $r_2$ and $R$ ) in secondary deformation zone

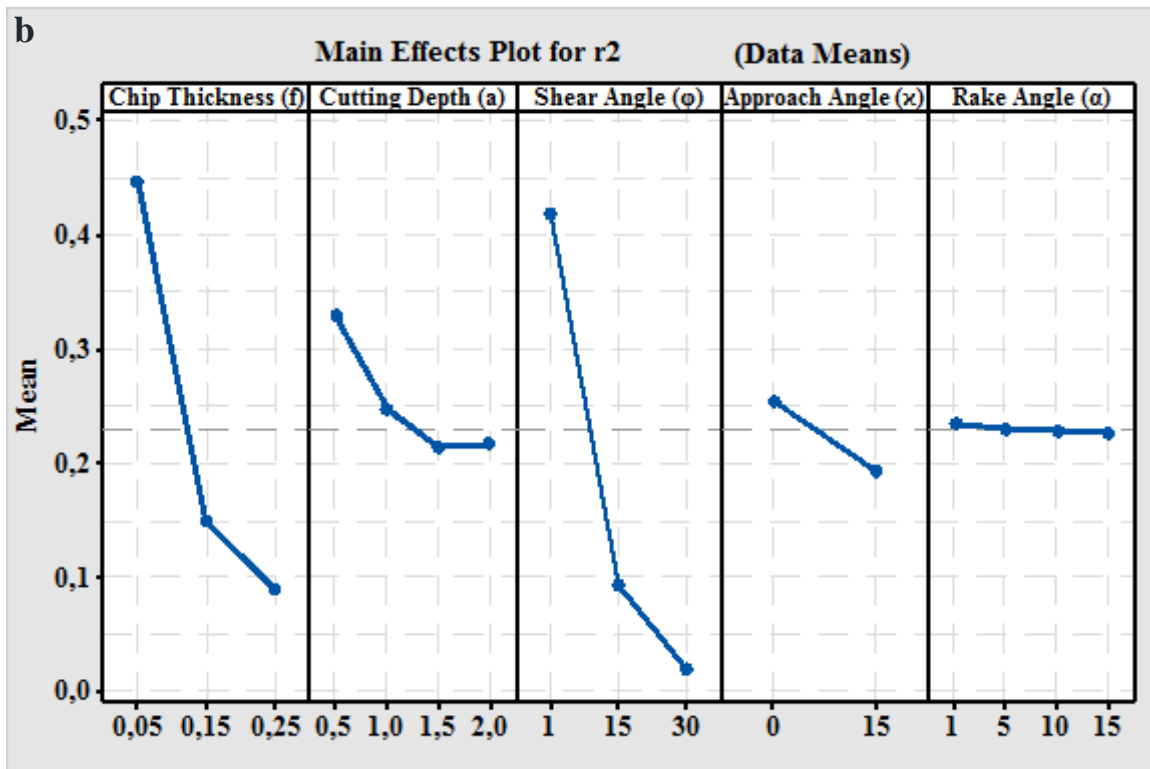
After the chip cut from the workpiece in primary deformation zone, then it moves on the rake face of the tool away, in secondary deformation zone. At the stage of secondary deformation zone the chip sustains to deformation by the effect of rake angle and deformation angle. According to the chip volumes, in Equations 9 and 14, the volumetric chip expansion factors ( $r_2$ ) and ( $R$ ) can be derived by dividing (V3) and (V4) to (V1), respectively, as seen in Equations 17 and 18. As seen in Figure 9 and 10 the changing of volumetric chip expansion factors ( $r_2$ ) and ( $R$ ) is too small. This means that the chip completed its expansion and deformation stage approximately in primary deformation zone, then it moves away on the rake face, in machining operations. However, the effect of shear angle, cutting edge approach angle and chip thickness is bigger than the effect of cutting depth and rake

angle, as in primary deformation zone. Although rake angle is prevail in secondary deformation zone, there is too small effect on the volumetric chip expansion factor to negligible.

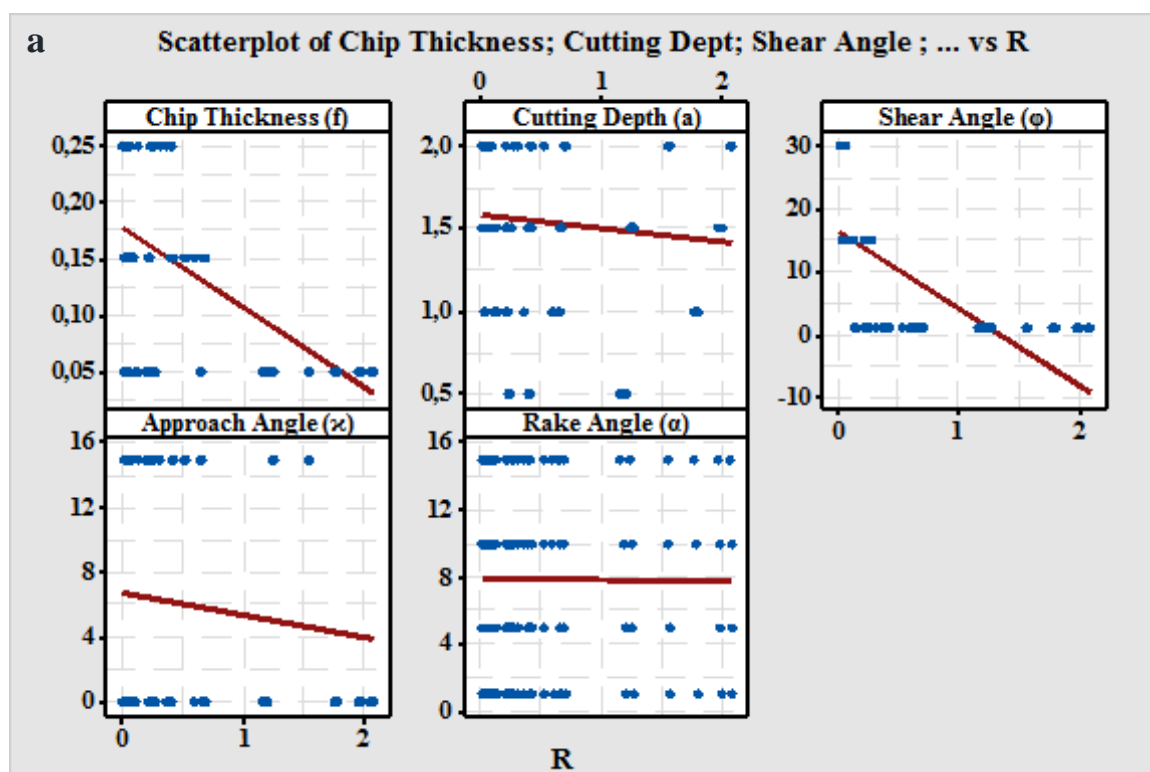
The effect of the most influential parameters, shear angle, chip thickness, and cutting edge approach angle, on volumetric chip expansion factor ( $r_2$ ), only changeable approximately one unit, as seen in Figure 9 a, b, and c, depending on scatter and main effect plots graphs, respectively.

When the chip moves on the rake angle, it sustains to deformation by the effect of deformation angle ( $\gamma$ ) as well. The effect of the deformation angle on volumetric chip expansion factor ( $R$ ) derivable by dividing (V4) to (V1). The effect of shear angle, cutting edge approach angle, and chip thickness on the volumetric chip expansion factor ( $R$ ) only changeable about 0.8 unit in maximum, as seen in Figure 10 a and b.





**Figure 9:** a) Scatterplot graphs, b) main effect plot of chip thickness, cutting depth, shear angle, approach angle, rake angle and chip expansion factor in the second deformation zone.



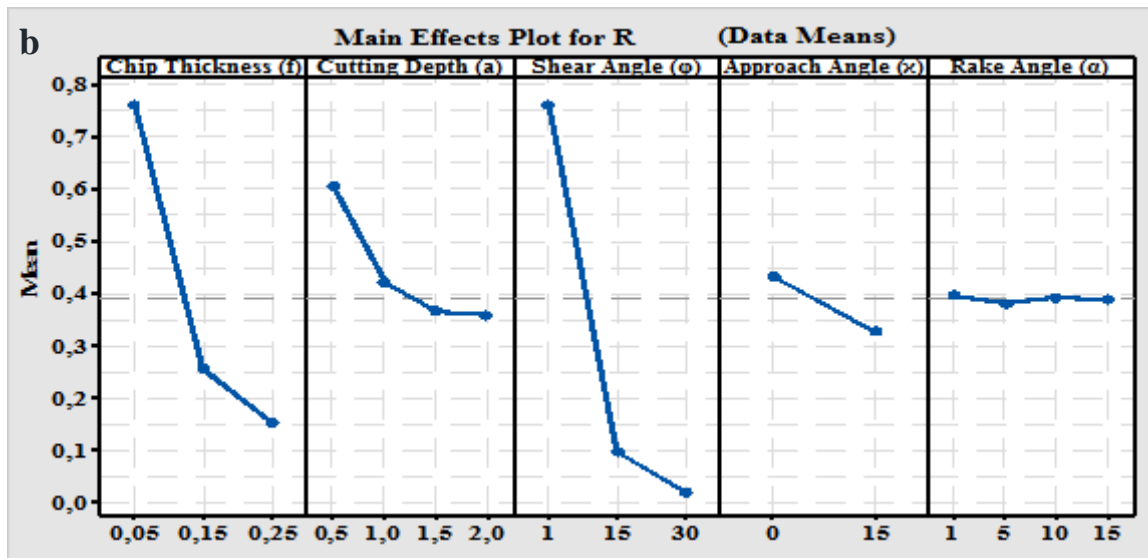


**Figure 10:** The effect of deformation angle on the chip expansion factor, a) Scatterplot graphs, b) main effect plot of chip thickness, cutting depth, shear angle, approach angle, rake angle and chip expansion factor in the second deformation zone.

#### 4. Conclusions

Volumetric chip expansion factor is a vital identifier for the machinability tests. For this purpose, the influential parameters, especially shear angle, tool cutting edge approach angle, chip thickness or feed rate, cutting depth or chip wide, and rake angle, on it was investigated geometrically, in this study. Finally, it was investigated that the most efficacious parameters on the volumetric chip expansion factor were shear angle, chip thickness, and tool cutting edge approach angle, but cutting depth and rake angle had not any important effect, in primary deformation zone.

Shear angle and chip thickness or feed rate had an inversely proportional severe effect on the volumetric chip expansion factor, but tool cutting edge approach angle had correlate effect. This mean for obtaining the optimum volumetric chip expansion factor values, higher shear angle and feed rates or chip thicknesses, but lower tool cutting edge approach angles must be selected.

The removed chip approximately completes its expansion in primary deformation zone mostly by the effect of shear angle, tool cutting edge angle, and feed rate. The effect of cutting depth is too small to negligible. Rake angle has not any effect on volumetric chip expansion factor both in primary and deformation zones. However, it affects the sliding of the removed chip on the rake face of the tool, which causes to increase the process temperature, due to the friction in the contacts area of tool-chip interface.

#### References

- [1] Arif, G. (2017) 2D numeric simulation of serrated-chip formation in orthogonal cutting of AISI316H stainless steel. *Materials and Technology*, 51 (6): 953 – 956.
- [2] Arrazola, P. J.; Villar, A.; Ugarte, D. (2007) Serrated chip prediction in finite element modeling of the chip formation process. *Machining Science and Technology*, 11: 367 – 390.
- [3] Ashwin, D.; Thomas, B.; Raveendra, S.; Ronnie, L.; Mahdi, E. (2017) Finite element modeling and validation of chip segmentation in machining of AISI 1045 steel. *Procedia CIRP*, 58:499 – 504.
- [4] Atlati, S.; Haddag, B.; Nouari, M.; Zenasni, M. (2011) Analysis of a new segmentation intensity ratio “SIR” to characterize the chip segmentation process in machining ductile metals. *International Journal of Machine Tools &Manufacture*, 51:687 – 700.
- [5] Bäker, M. (2003) An investigation of the chip segmentation process using finite elements. *Technische Mechanik*, 23 (1): 1 – 9.
- [6] Buchkremer, S.; Schoop, J. (2016) A mechanics-based predictive model for chip breaking in metal machining and its validation. *CIRP Annals – Manufacturing Technology*, 65:69 – 72.
- [7] Gao, C.; Zhang, L. (2013) Effect of cutting conditions on the serrated chip formation in high-speed cutting. *Machining Science and Technology*, 17: 26 – 40.

- [8] Ijaz, H.; Zain-ul-abdein, M.; Saleem, W.; Asad, M.; Mabrouki, T. (2017) Numerical simulation of the effects of elastic anisotropy and grain size upon the machining of AA2024. *Machining Science and Technology*, 0 (0): 1 – 21.
- [9] Kishawy, H. A.; Rogers, R. J.; Balihodzic, N. (2002) A numerical investigation of the chip tool interface in orthogonal machining. *Machining Science and Technology*, 6 (3): 397 – 414.
- [10] Lampart, P. (2009) Investigation of endwall flows and losses in axial turbines. Part II. The effect of geometrical and flow parameters. *Journal of Theoretical and applied mechanics*, 47 (4): 829 – 853.
- [11] Liu, R.; Elijah, E.; Mendy, Y.; Kuang, J. (2017) An investigation of side flow during chip formation in orthogonal cutting. *Procedia Manufacturing*, 10: 568 – 577.
- [12] Michael, K. (1996) *Machining science and application theory and practice for operation and development of machining processes*. Arrowsmit Ltd. UK. 3 – 18.
- [13] Miguelez, M. H.; Sanchez, A. M.; Cantero, J. L.; Loya, J. A. (2009) An efficient implementation of boundary conditions in an ale model for orthogonal cutting. *Journal of Theoretical and applied mechanics*, 47 (3): 599 – 616.
- [14] Mustafa, A. (1996) *Machining methods and machine tools*. 3rd Edition, Birsen Press, İstanbul, Turkey, 23-26.
- [15] Uçun, İ.; Aslantas, K.; Fevzi, B. (2016) Finite element modeling of micro-milling: Numerical simulation and experimental validation. *Machining Science and Technology*, 20 (1): 148 – 172.
- [16] Weber, M.; Hochrainer, T.; Gumsch, P.; Autenrieth, H.; Dellonoy, L.; Schulze, V.; Löhe, D.; Kotschenreuther, J.; Fleischer, J. (2007) Investigation of size-effects in machining with geometrically defined cutting edges. *Machining Science and Technology*, 11: 447 – 473.
- [17] Ye, G. G.; Chen, Y.; Xue, S. F.; Dai, L. H. (2014) Critical cutting speed for onset of serrated chip flow in high speed machining. *International Journal of Machine Tools & Manufacture*, 86: 18 – 33.
- [18] Ye, G. G.; Jiang, M. Q.; Xue, S. F.; Ma, W.; Dai, L. H. (2018) On the stability of chip flow in high-speed machining. *Mechanics of Materials*, 116: 104 – 119.

### Author Profile



**Zülküf DEMİR** received the B.S. and M.S. degrees in Mechanical Educational and Engineering from Dicle and Atatürk Universities in 2003 and 2012, respectively. During 1999-2012, he worked as a technical teacher at different technical high schools in Turkey. Since 2013 he has been working at Batman University as an academician, in the area of Mechanical Engineering Department.